

Evidence of Variable H-Bond Network for Nitroxide Radicals in Protic Solvents

Michele Pavone, Atte Sillanpää,[†] Paola Cimino,[‡] Orlando Crescenzi, and Vincenzo Barone**Dipartimento di Chimica, Università di Napoli Federico II, Complesso Universitario di Monte Sant'Angelo, Via Cintia, I-80126 Napoli, Italy**Received: June 21, 2006; In Final Form: July 20, 2006*

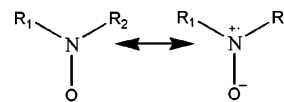
This letter presents the results of a thorough computational investigation of two prototypical nitroxide spin probes in two different protic solvents, namely water and methanol, based on the combined use of Car–Parrinello molecular dynamic simulations and static cluster/continuum quantum chemical computations. Remarkable changes in solvation networks were found on going from aqueous to methanolic solutions. Moreover, despite their structural similarity, the two nitroxide probes display quite different behaviors in water. This provides a rationalization of indirect experimentally available indications. Eventually, the combination of static and dynamical *ab initio* methods exploited in the present study allows to dissect many subtle features of the nitroxide–solvent interaction, and also allows for an analysis of solvent effects on magnetic parameters (hyperfine coupling constants and *g*-tensor shift).

Nitroxide free-radicals present an unusually stable doublet ground state,¹ in which the spin-density is essentially localized on the NO moiety. The relative chemical inertness of the nitroxyl functional group, coupled with its sensitivity to the chemical surroundings, has motivated a widespread application of nitroxide compounds as spin probes for electronic spin resonance (ESR)² in a variety of chemical investigations.^{3–6} The key point behind such applications is the interaction of a nitroxide free-radical with its chemical environment, which results in a highly sensitive response of its structural, chemical, and spectroscopic properties.⁷ In connection with the interpretation of spectroscopic data, many experimental and theoretical efforts⁸ have been devoted to elucidate the relationships between the physico-chemical features of nitroxide radicals and the solvent medium employed. Qualitatively, the solvent dependence of nitroxide ESR parameters, e.g., nitrogen hyperfine coupling constant (*hcc*) and electronic *g*-tensor, has been ascribed to a selective stabilization of the charge-separated canonical structure of the NO functional group (Scheme 1).

An increased contribution of this form entails a larger spin density on nitrogen, and, in view of the spin–orbit coupling constant of nitrogen being smaller than that of oxygen, results in an increase of *hcc* and a decrease of *g*-value. However, solvent polarity and formation of solute–solvent hydrogen bonds play a synergic effect, so that the relationship between macroscopic observables and microscopic structure and dynamics are not straightforward, and theoretical models are crucial for a correct understanding of the complex experimental data.^{8,9}

The present contribution is devoted to a thorough computational analysis of specific solvent–nitroxide interactions, based on a combination of first-principle molecular dynamics (MD) simulations and cluster-continuum approaches rooted in the

SCHEME 1: Resonance Forms of the Nitroxyl Group



framework of density functional theory (DFT).¹⁰ In particular, we explored the strength and the geometrical features of the H-bond interaction of a five-membered cyclic nitroxide of widespread use as a spin probe, namely 2,2,5,5-tetramethyl-1-pyrrolidinyloxy (hereafter “proxyl”, see Figure 1) in two common protic solvents, water and methanol. Despite the apparent similarity of the two solvents, our computations reveal a marked difference in the structure of the H-bonding network around the NO moiety. Furthermore, the aqueous solution behavior of proxyl has been compared with that of a more flexible nitroxide molecule, bis(1,1-dimethylethyl)nitroxide, commonly known as di-*tert*-butylnitroxide (hereafter “dtbn”, see Figure 1).¹¹ Once again, our results provide a quite different picture for the two H-bonding networks, thus highlighting, on another perspective, a significant dependence upon solute molecular parameters.

To overcome the limitations of currently available empirical force fields for organic free radicals, we performed Car–Parrinello (CP)¹² MD simulations, using the gradient-corrected density functional of Perdew, Burke, and Ernzerhof (PBE)¹³ under the conditions detailed in the Supporting Information.

A first rough indication of the average number of hydrogen bonds between proxyl oxygen and solvent molecules is obtained by integrating the first peaks of the radial distribution functions (RDFs), depicted in Figure 2. The average number of solvent molecules coordinating the nitroxyl moiety is around two for the aqueous solution, but is close to one in the case of methanol. To make sure that the single methanol–proxyl H-bond was not an artifact of the limited statistics of CPMD, we generated a second trajectory starting from a configuration with two

* Corresponding author. E-mail: baronev@unina.it

[†] Permanent address: CSC—Scientific Computing Ltd., Espoo, Finland.[‡] Permanent address: Dipartimento di Scienze Farmaceutiche, Università di Salerno, Fisciano (SA), Italy.

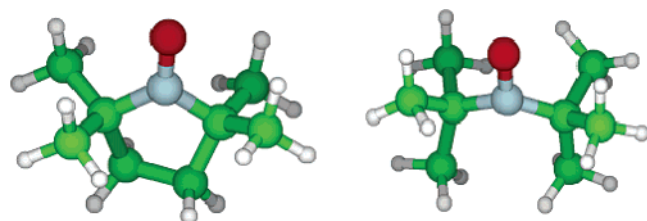


Figure 1. Nitroxide molecular structures: proxyl on the left and dtbn on the right.

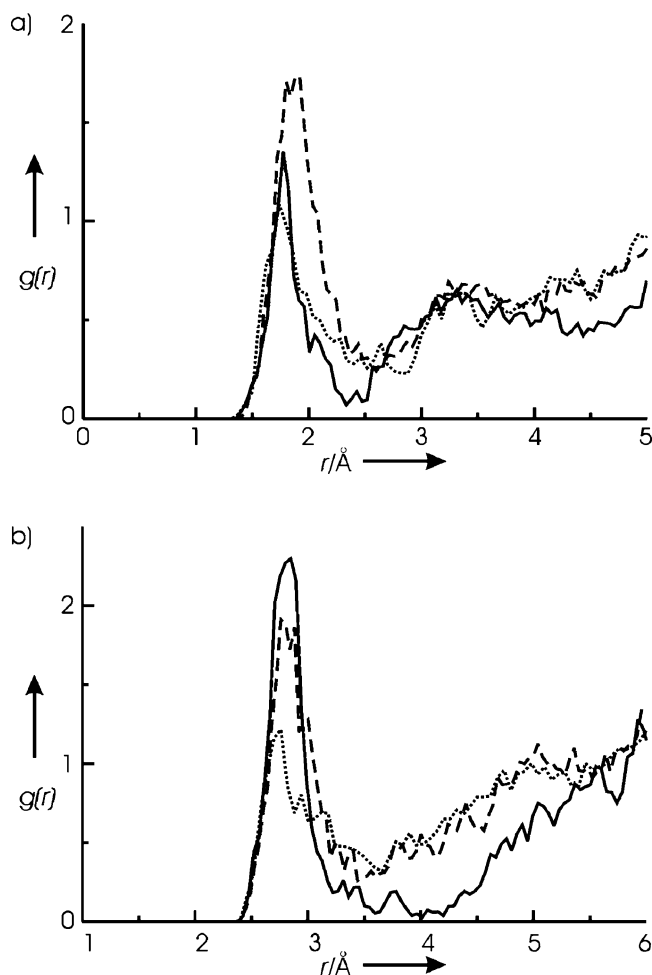


Figure 2. Radial distribution functions: (a) $O_{\text{solute}} - H_{\text{solvent}}$ and (b) $O_{\text{solute}} - O_{\text{solvent}}$; full line, proxyl in methanol; dashed line, proxyl in water; dotted line, dtbn in water.

methanol–nitroxide H-bonds; however, after few picoseconds one of the solvent molecules leaves the first coordination shell of the nitroxide oxygen. Further insight was sought by adopting a set of purely structural criteria¹⁴ to compute the number of H-bonds and to measure their average geometries: data are listed in Table 1. In the comparison between methanolic and aqueous solution, the average molecular structure of the nitroxide is essentially unperturbed, and also the structural features of the hydrogen bonds are quite similar, as is the position of the first peaks of the RDFs. The average number of proxyl–solvent H-bonds computed by the geometrical criteria is consistent with that obtained by integration of the RDFs; the higher standard deviation of the parameters associated to water–nitroxide H-bonds could be indicative of higher solvent mobility. Figure 3 shows the percentage of configurations sampled along the CPMD trajectories that display a definite number of H-bonds: the vast majority (over 90%) of the frames from the methanol

TABLE 1: Average Geometrical Parameters Extracted from the CPMD Trajectories^a

| parameter | proxyl | | dtbn |
|-------------------------------------|---------------------|------------------|------------------|
| | methanolic solution | aqueous solution | aqueous solution |
| N–O | 1.30 (0.02) | 1.30 (0.02) | 1.31 (0.02) |
| C–N–C | 114 (2) | 115 (2) | 127 (4) |
| Abs(C–N–O···C) | 166 (9) | 167 (9) | 170 (8) |
| no. of H-bonds ^b | 1.0 (0.2) | 1.9 (0.7) | 1.2 (0.5) |
| $O \cdots O_{\text{solvent}}^c$ | 2.8 (0.2) | 2.9 (0.2) | 2.9 (0.2) |
| $O \cdots H_{\text{solvent}}^c$ | 1.9 (0.2) | 2.0 (0.2) | 1.9 (0.3) |
| $O \cdots O - H_{\text{solvent}}^c$ | 12 (6) | 15 (7) | 15 (7) |

^a Distances in Angstroms, angles in degrees, standard deviations in parentheses. ^b $O \cdots O_{\text{solvent}} \leq 3.5$ Å; $O \cdots H_{\text{solvent}} \leq 2.6$ Å; $O \cdots O - H_{\text{solvent}} \leq 30^\circ$. ^c Averaged over solvent molecules H-bonded to the nitroxide.

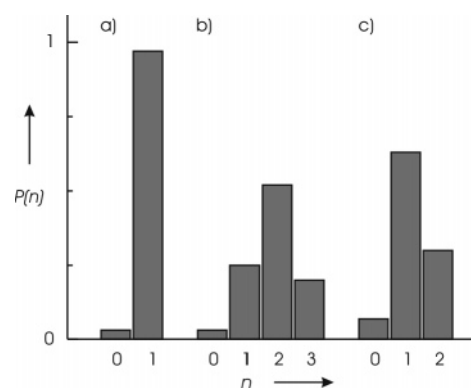


Figure 3. Number of solute–solvent H-bonds along the CPMD trajectories for (a) proxyl in methanol, (b) proxyl in water, and (c) dtbn in water.

simulation present one H-bond, and a small fraction present no H-bond at all; on the other hand, in aqueous solution more than half of the frames have two genuine water–nitroxide H-bonds; configurations with just one or with three H-bonds are also represented, while the fraction of frames lacking any H-bond is small. Overall, the geometrical analysis confirms the change in average number of solvent molecules coordinating the nitroxyl moiety, from two in aqueous solution to one in methanol.

Table 1 and Figure 3 collect also the results issuing from a similar analysis of a CPMD dynamics of dtbn in aqueous solution, carried out under the same conditions as for proxyl. Unexpectedly, the probability of achieving two genuine H-bonds is now much lower than for a single H-bond.

In summary, the first-principle trajectories of two similar spin-probe prototypes in water present a surprisingly variable H-bonding network depending on the structure of the solute; a drastic change in average number of H-bonds is also observed for the five-membered ring nitroxide when the solvent is changed from water to methanol.

To gain further insight into the results from the CP dynamics, we resorted to a quantum-chemical analysis of the interaction energies of nitroxide–solvent clusters, employing the hybrid density functional known as PBE0,¹⁵ under the conditions detailed in the Supporting Information.

Energy minima of the proxyl-*n* (solvent) clusters (*n* = 1, 2) have been computed in the gas-phase; isolated solvent molecules, as well as solvent–solvent clusters, were also examined for comparison (Cartesian coordinates of all the optimized structures are given in the Supporting Information). To take into proper account the effect of the solvent beyond the few molecules explicitly represented in the cluster, single point energies of the solute–solvent clusters were also computed by

TABLE 2: Interaction Energies [$E = E_{\text{nitroxide}-n(\text{solvent})} - E_{\text{nitroxide}} - n(E_{\text{solvent}})$; $n = 1, 2$] in kcal mol⁻¹

| cluster | gas phase ^a | solution (PCM) ^a |
|-------------------------------|------------------------|-----------------------------|
| proxyl-H ₂ O | -7.0 | -1.7 |
| proxyl-2 (H ₂ O) | -13.2 (-6.2) | -2.2 (-0.5) |
| proxyl-CH ₃ OH | -7.0 | -0.4 |
| proxyl-2 (CH ₃ OH) | -13.1 (-6.1) | 0.5 (0.9) |
| dtbn-H ₂ O | -5.7 | -1.4 |
| dtbn-2 (H ₂ O) | -12.3 (-6.6) | -0.5 (0.9) |

^a The separate contribution of the second H-bond is given in parentheses.

using the polarizable continuum model (PCM)¹⁶ in its UAHF parametrization.¹⁷ Such a discrete-continuum solvation model¹⁸ has been tested and validated for many nitroxide–water^{8b} and nitroxide–alcohol systems.¹⁹ Table 2 lists the computed interaction energies.

Both proxyl–water and proxyl–methanol optimized clusters present, in the gas phase, a first H-bond with a stabilization energy of ~7 kcal/mol; the energy gain for the second H-bond is slightly lower, ~6 kcal/mol, resulting in a total interaction energy (with respect to isolated proxyl and solvent molecules) of approximately -13 kcal/mol. Thus, at this level of analysis, the intermolecular interactions with water and with methanol are similar and apparently do not correlate with the change in average number of H-bonds observed in the CPMD runs. However, inclusion of the remaining solvent degrees of freedom, i.e., bulk dielectric and short-range nonelectrostatic contributions, by means of the PCM solvation model, provides a quite different picture. In aqueous solution, both the first and the second H-bond between water and proxyl are energetically favorable, with a gain of 1.7 and 0.5 kcal/mol, respectively; apart from the smaller absolute energies involved, the results from the gas-phase cluster analyses are confirmed. On the other hand, in methanol solution only the first methanol–nitroxide H-bond is favorable (-0.4 kcal/mol); the adduct with two methanol molecule H-bonded to the nitroxide oxygen, that was stable in the gas phase, becomes unstable, with a total interaction energy of +0.5 kcal/mol. Thus, when solvent effects are accounted for by a cluster-PCM approach, two genuine H-bonds are predicted to exist in water, but only one in methanol, a picture that fits nicely with the results from the CPMD trajectories.

A parallel analysis of dtbn in water also provides results in agreement with the H-bonding network observed in the CPMD simulation. Briefly, when examined in solution (PCM), only the first H-bond between water and dtbn is energetically favored.

Steric effects are probably crucial in determining the observed behavior of the systems (see molecular structures in Figure 1). In proxyl, the four methyl groups determine an accessible region around the nitroxyl that is ample enough to easily accommodate two hydrogen-bonded water molecules, but is essentially exhausted by the first methanol molecule.²⁰ In the acyclic dtbn, the conformational freedom of the methyl groups is definitely larger; moreover, repulsive intramolecular interactions between the two *tert*-butyl moieties cause a marked widening of the C–N–C angle (127° in the average, versus 115° in proxyl); as a result, the region around the nitroxyl group is even more crowded than in proxyl, and interaction with a second solvent molecule becomes unfavorable even with water.

Apart from structural parameters, a particularly useful comparison with experimental data can be obtained by computing nitrogen hyperfine coupling constants (A_N) and shifts of the electronic g-tensor (Δg) for proxyl and proxyl–solvent adducts with bulk solvent effects modeled by the PCM. In this case the

TABLE 3: Solvent Shifts of Nitrogen Hyperfine Coupling Constant (ΔA_N in Gauss) and g-value ($\Delta \Delta g$ in ppm) Computed for Proxyl in Different Solutions

| molecule/cluster ^a | aqueous solution | | methanolic solution | |
|-------------------------------|------------------|-------------------|---------------------|-------------------|
| | ΔA_N | $\Delta \Delta g$ | ΔA_N | $\Delta \Delta g$ |
| proxyl | 0.98 | -176 | 0.95 | -170 |
| proxyl-S | 1.70 | -370 | 1.66 | -367 |
| proxyl-2 S | 2.29 | -523 | 2.28 | -536 |

^a S = H₂O and CH₃OH for aqueous and methanolic solutions, respectively.

PBE0 density functional has been employed in combination with the purposely tailored EPR-II basis set.²¹ The suitability of the protocol for the computation of anisotropic terms has been shown previously;^{11a,22} however, in the present context we will concentrate on the isotropic terms, which are the most relevant for the interpretation of standard solution spectra. The overall solvent shifts of the magnetic parameters (Table 3) are in agreement with their experimental counterparts.^{8,23} For instance, the experimental solvent shift for the A_N of proxyl between water and dodecane solutions is 2.35 G,²³ and that between methanol and water solutions for a closely related nitroxide is 1.01 G.^{22,24} From another point of view, bulk solvent effects and short-range H-bonding contributions are comparable in aqueous and methanolic solutions. Thus, the differences observed in experimental ESR data should be mainly due to differences in the solvent network embedding the nitroxide oxygen, rather than to the dielectric constant.

In conclusion, our analysis of the nitroxide–methanol and nitroxide–water H-bonding network by state-of-the-art first-principle methods points out that, from both dynamic and static perspectives, the solvation structure of prototypical, real-size spin probes depends in a sensitive way on the nature of the solvent, as well as on the structure of the solute. Our methodology, directly concerned with relatively fast and local solvent motions, highlights the importance of careful computational modeling for the interpretation of experimental data on the behavior of nitroxide spin probes and represents a significant step in the general direction of a truly multiscale approach to the ab initio interpretation of ESR line shapes in water and other protic environments.

Supporting Information Available: Computational details are available free of charge via the Internet at <http://pubs.acs.org>.

References and Notes

- (1) Keana, J. F. W. *Chem. Rev.* **1978**, *78*, 37.
- (2) Stone, T. J.; Buckman, T.; Nordio, P. L.; McConnell, H. *Proc. Natl. Acad. Sci. U.S.A.* **1965**, *54*, 1010.
- (3) Buchaklian, A. H.; Klug, C. S. *Biochemistry* **2005**, *44*, 5503.
- (4) Lucarini, M.; Franchi, P.; Pedulli, G. F.; Pengo, P.; Scrimin, P.; Pasquato, L. *J. Am. Chem. Soc.* **2004**, *126*, 9326.
- (5) Tedeschi, A. M.; D'Errico, G.; Busi, E.; Basosi, R.; Barone, V. *Phys. Chem. Chem. Phys.* **2002**, *4*, 2180.
- (6) Nicolas, J.; Charleux, B.; Guerret, O.; Magnet, S. *Angew. Chem., Int. Ed. Engl.* **2004**, *43*, 6186.
- (7) (a) Berliner, L. J.; *Spin Labeling, Theory and Applications*, Academic Press: New York, 1976. (b) Steinhoff, H.-J.; Savitsky, A.; Wegener, C.; Pfeiffer, M.; Plato, M.; Möbius, K. *BBA-Bioenergetics* **2000**, *1457*, 253. (c) Kurad, D.; Jenske, G.; Marsh, D. *Biophys. J.* **2003**, *85*, 1025.
- (8) (a) Knauer, B. R.; Napier, J. J. *J. Am. Chem. Soc.* **1976**, *91*, 4395. (b) Improta, R.; Barone, V. *Chem. Rev.* **2004**, *104*, 1231.
- (9) Wu, D. G.; Malec, A. D.; Head-Gordon, M.; Majda, M. *J. Am. Chem. Soc.* **2005**, *127*, 4490.
- (10) (a) Hohenberg, P.; Kohn, W. *Phys. Rev.* **1964**, *136*, B864. (b) Kohn, W.; Sham, L. J. *Phys. Rev.* **1965**, *140*, A1133.
- (11) (a) Mattar, S. M.; Stephens, A. D.; *Chem. Phys. Lett.* **2001**, *347*, 189. (b) Pavone, M.; Cimino, P.; De Angelis, F.; Barone, V. *J. Am. Chem. Soc.* **2006**, *128*, 4338.

- (12) Car, R.; Parrinello, M. *Phys. Rev. Lett.* **1985**, *55*, 2471.
- (13) Perdew, J. P.; Burke, K.; Ernzerhof, M. *Phys. Rev. Lett.* **1996**, *77*, 3865.
- (14) Pavone, M.; Benzi, C.; De Angelis, F.; Barone, V. *Chem. Phys. Lett.* **2004**, *395*, 120.
- (15) Adamo, C.; Barone, V. *J. Chem. Phys.* **1999**, *110*, 6158.
- (16) Miertus, S.; Scrocco, E.; Tomasi, J. *Chem. Phys.* **1981**, *55*, 117.
- (17) Cossi, M.; Scalmani, G.; Rega, N.; Barone, V. *J. Chem. Phys.* **2002**, *117*, 43.
- (18) (a) Persico, M.; Tomasi, J. *Chem. Rev.* **1994**, *94*, 2027. (b) Cramer, C. J.; Truhlar, D. G. *Chem. Rev.* **1999**, *99*, 2161. (c) Tomasi, J.; Mennucci, B.; Cammi, R. *Chem. Rev.* **2005**, *105*, 2999.
- (19) Cimino, P.; Pavone, M.; Barone, V. *Chem. Phys. Lett.* **2006**, *419*, 106.
- (20) Romanelli, M.; Ottaviani, M. F.; Martini G.; Kevan, L. *J. Phys. Chem.* **1989**, *93*, 317.
- (21) Barone, V. *Theor. Chim. Acta* **1995**, *91*, 113.
- (22) (a) Owenius, R.; Engström, M.; Lindgren M.; Huber, M. *J. Phys. Chem. A* **2001**, *105*, 10967. (b) Ciofini, I.; Barone, V.; Adamo, C. *J. Chem. Phys.* **2004**, *121*, 6710. (c) Sinnecker, S.; Rajendran, A.; Klamt, A.; Diedenhofen, M.; Neese, F. *J. Phys. Chem. B* **2006**, *110*, 2235.
- (23) Keana, J. F. W.; Lee, T. D.; Bernard, E. M. *J. Am. Chem. Soc.* **1976**, *98*, 3025.
- (24) Reddoch, A. H.; Konishi, S. *J. Chem. Phys.* **1979**, *70*, 2121.